Journal of Magnetics 16(3), 304-307 (2011) http://dx.doi.org/10.4283/JMAG.2011.16.3.304

Effect of Microstructure on the Corrosion Resistance of Nd-Fe-B Permanent Magnets

Jiajie Li*, Wei Li, Anhua Li, Rui Zhao, Bin Lai, and Minggang Zhu

Division of Functional Materials, Central Iron and Steel Research Institute, Beijing 100081, China

(Received 6 July 2011, Received in final form 8 August 2011, Accepted 9 August 2011)

High performance Nd-Fe-B magnets can be manufactured by both sintering and hot deformation. The corrosion behaviors of the magnets prepared by the two processes were compared. Effect of microstructure on the corrosion resistance of Nd-Fe-B magnets was also investigated. A neutral salt spray test (NSS) was performed for the different-processed magnets. The weight losses of the samples after the corrosion test were measured. The corrosion microstructures were observed using a scanning electron microscope. It shows that the corrosion resistance of hot deformed magnets is much better than that of the sintered ones because the grain size and the distribution of Nd-rich phases of the hot deformed magnets are much finer and more uniform than those of the sintered ones. The different microstructure between the sintered and the hot deformed magnets causes the different corrosion behavior.

Keywords : Nd-Fe-B magnets, sintering, hot deformation, microstructure, corrosion resistance

1. Introduction

Nd-Fe-B magnets possessing outstanding magnetic properties are widely applied in many fields. However, corrosion resistance has been a problem with the Nd-Fe-B magnets owing to the high chemical activity of the phases rich in rare earth elements [1]. The Nd-rich phases on the surface of the magnets can react with water vapor and oxygen in a damp and humid atmosphere. The reaction resultant of H then diffuses into the grain boundaries, reacts with the Nd-rich phases to form NdH_3. The NdH_3 causes a volume expansion of the grain boundary phase, so creates a local stresses which lead to the spalling of the matrix $Nd_2Fe_{14}B$ grains [2, 3]. Because the corrosion potential is different between the matrix $Nd_2Fe_{14}B$ phase and the boundary Nd-rich phase, the corrosion micro-battery forms, and therefore the electro-chemical corrosion occurs for Nd-Fe-B magnets in a high humidity atmosphere when water (such as the little liquid droplets) exists on the surface of the magnet [4].

High performance Nd-Fe-B magnets can be manufactured by both sintering and hot deformation. These differently processed magnets have obviously different microstructures. In this article, we compared the corrosion behaviors of Nd-Fe-B magnets prepared by sintering and by hot deformation. Effect of microstructures on the corrosion resistance of Nd-Fe-B magnets was also investigated.

*Corresponding author: Tel: +86-10-62185854
Fax: +86-10-62182610, e-mail: lifest@163.com

2. Experiments

The chemical compositions of experimental Nd-Fe-B magnets are listed in Table 1. The sample A with high $(BH)_{max}$, and sample B with high H_{cj} were prepared by the conventional sintering process. The sample H was obtained by hot deforming the pressed precursor of melt-spun nanocrystalline powders. The corrosion behaviors of these magnet samples were investigated by a neutral salt spray test (NSS) using 5 wt.% sodium chloride solution at 35 °C. After corrosion testing, the weight loss of the

Table 1. Chemical compositions of experimental Nd-Fe-B magnets (wt.%).

Sample No.	Al	B	Co	Cu	Ga	Dy	Nd	Fe
A	0.09	0.99	0.5	0.16	0.11	0.18	27.91	68.93
B	0.47	0.97	2.11	0.22	0.1	8.78	22.27	65.03
H	–	0.95	4.0	–	0.5	–	30.0	64.55

samples was measured after brushing off the corrosion products. A LEO-1450 scanning electron microscope (SEM) equipped with an energy-dispersive X-ray spectroscopy (EDS) were employed to observe the microstructures of the corroded samples.

3. Results and Discussion

The weight losses of the magnet samples after the NSS test are shown in Fig. 1. The curves of weight loss vs. test time approximately show the parabolic waveforms for both the sintered samples A and B, and the hot deformed sample H. It is found that the weight losses for all samples are very small in the initial stage of NSS test, nearly keep invariable until the test time of 40 hours. This is because only the surface-layer oxidations occur in the magnets during this stage. Consequently, the weight losses of the samples enhanced with increasing test time *t*, due to the preferential corrosion of intergranular phases accompanied by the spalling of the matrix $Nd_2Fe_{14}B$ phases from the magnet surface [5]. After the NSS test for 110 hours, the weight losses of samples A and B are 42.79 mg·cm^{-2}, and 21.98 mg·cm^{-2}, respectively, while sample H has the weight loss of 9.85 mg·cm^{-2}. It can be seen that the weight loss of the hot deformed sample H is much smaller than that of the sintered samples A and B, therefore the hot deformed sample has the best corrosion resistance among these tested samples. For the sintered magnets, sample B with higher Dy and Co contents has better corrosion resistance than sample A.

The corrosion macro- and micromorphologies of the tested samples were studied. The brown corrosion products and some corrosion pits were found in the surface of the samples after the NSS test for 110 hours. The typical SEM micromorphologies of the magnet samples after the NSS test are shown in Fig. 2. Compared with the sintered samples (sample B), the corrosion surface of the hot deformed sample H is relatively even. The amount of the corrosion products brushed off from the surface of sample H is much less than that from sintered ones. It is also confirmed by the weight losses of the tested samples (see Fig. 1). The deep corrosion holes and wide cracks can be observed in the surface of sintered samples, but only the superficial pits and narrow cracks can be seen in the surface of hot deformed ones.

The different corrosion behaviors between the hot deformed and the sintered magnets are mainly caused by their different microstructures. As shown in Fig. 3, the grain size and the distribution of Nd-rich phases for hot deformed magnets are much finer and more uniform than those of the sintered one (sample B). The hot deformed Nd-Fe-B magnets show platelet-shaped grains, and the grain dimension perpendicular to the compressive stress is about 200-300 nm, while the dimension parallel to the compressive stress is about 30-50 nm. The sintered magnets have particle-shaped grains with a diameter of about

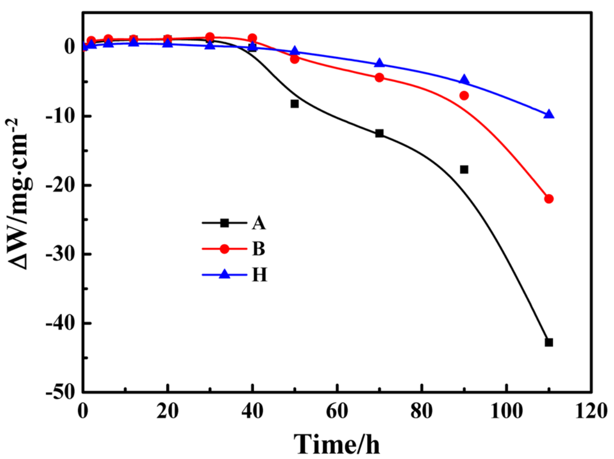

Fig. 1. (Color online) Weight losses of the sintered (samples A and B) and the hot deformed Nd-Fe-B magnets (sample H) after the NSS test for different time.

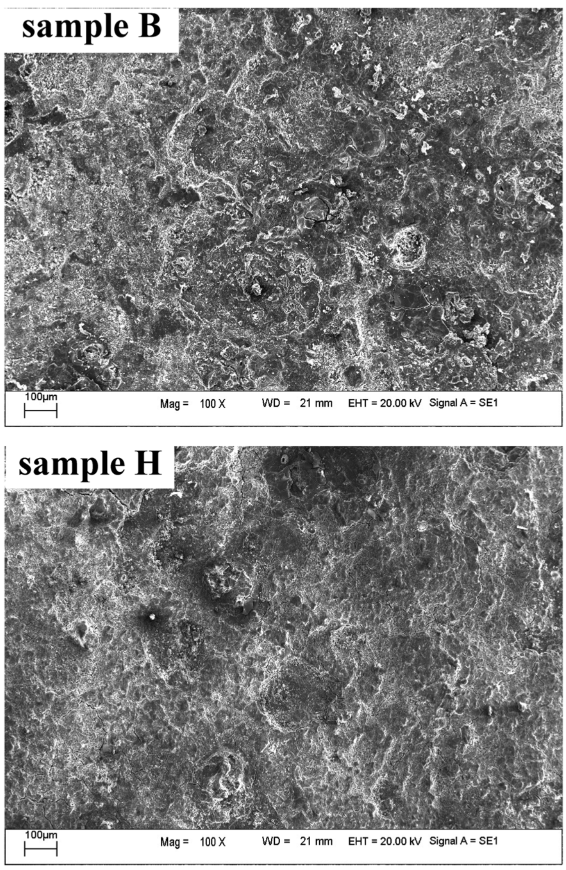

Fig. 2. Corrosion micromorphologies of the sintered (sample B) and the hot deformed Nd-Fe-B magnets (sample H) after the NSS test.

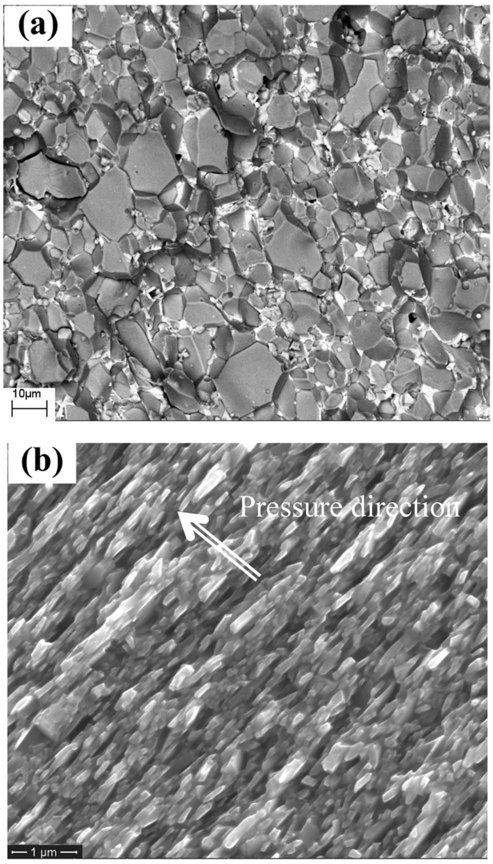

Fig. 3. SEM micrographs of the sintered (a) and the hot deformed (b) Nd-Fe-B magnets.

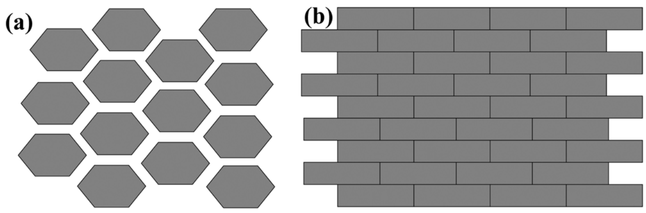

Fig. 4. Sketch maps of the microstructures of the sintered (a) and the hot deformed (b) Nd-Fe-B magnets.

10 μm. Sintered Nd-Fe-B magnets are mainly composed of the matrix $Nd_2Fe_{14}B$ phases surrounded by the chemically active Nd-rich phases with a network structure. The microstructural illustrations of Nd-Fe-B magnets prepared by sintering and hot deformation are shown in Fig. 4.

The hot deformed magnet has a nano-grained microstructure, and is more compact than the sintered one because of their different preparing processes. Both the oxygen in air and chloride ions in salt fog are not easy to diffuse into the base of the compact hot deformed magnet, so the hot deformed magnet has better corrosion resistance. The chloride ions serve as activator and play an important role in the neutral salt spray corrosion testing. Chloride elements were found in the surface of tested samples by EDS analyses. For the sintered Nd-Fe-B magnets, their poor corrosion-resistance is mainly caused by the Nd-rich boundary phases with the high chemical activity and the network structure.

It is thought that the O_2 and Cl^- can diffuse along the grain boundaries into the interior of Nd-Fe-B magnets, react with Nd-rich phases inside, and so intergranular corrosion occurs. Consequently, the matrix $Nd_2Fe_{14}B$ phases separate from the magnet surface. An on-going corrosion will proceed in the sintered magnets, which lead to a larger weight losses in the NSS climate. Owing to the microstructure of platelet grains in the hot deformed magnets, the proceeding of the corrosion behavior maybe hindered, and it is difficult to reach the next layer. Furthermore, the grain boundary Nd-rich phases are much finer and disperse in the deformed magnets, which is a great benefit to their corrosion resistance. Therefore, the weight losses of the hot deformed sample are much less than those of the sintered ones in the NSS climate.

Nd-Fe-B magnets are characterized by intergranular corrosion [6]. The substitutions of Dy for Nd, and Co, Ga for Fe can substantially improve the corrosion resistance of Nd-Fe-B magnets in the NSS climate because some of new phases, such as the Dy and Co-rich phases, Nd_3Co, etc, are formed in the boundary [7]. The chemical activity of the boundary phases is reduced, and thus the corrosion resistance of the magnets is simultaneously improved.

4. Conclusions

In this article, we compared the corrosion behavior of Nd-Fe-B magnets prepared by the sintering and the hot deformation. Effect of microstructures on the corrosion resistance of Nd-Fe-B magnets has been discussed. The hot deformed magnets exhibit much better corrosion resistance than the sintered ones in the neutral salt spray test. It is because the hot deformed magnets have the microstructure of platelet-shaped nano-grains, where the grain boundary Nd-rich phases are much fine and disperse. The substitutions of Dy for Nd, and Co for Fe can substantially improve the corrosion resistance of sintered Nd-Fe-B magnets in the NSS climate.

Acknowledgements

This work is supported by the National Natural Science Foundation of China (50804011, 50871032) and the National High Technology Research and Development Program of China.

References

[1] D. F. Cygan and M. J. McNallan, J. Magn. Magn. Mater. **139**, 131 (1995).

[2] A. S. Kim, F. E Camp, and T. Lizzi, J. Appl. Phys. **79**, 4840 (1996).

[3] M. Katter, L. Zapf, and R. Blank, IEEE Trans. Magn. **37**, 2474 (2001).

[4] G. L. Yan, P. J. McGuiness, J. G. Farr, and I. R. Harris, J. Alloys Compd. **478**, 188 (2009).

[5] A. A. El-Moneim and A. Gebert J. Appl. Electrochem. **33**, 795 (2003).

[6] W. Q. Liu, M. Yue, and C. Y. Liu, J. Appl. Phys. **103**, 07E108 (2008).

[7] J. Fidler and T. Schrefl, J. Appl. Phys. **79**, 5029 (1996).